Wrinkling Phenomena in Neo-Hookean Film/Substrate Bilayers

Wrinkling phenomena in neo-Hookean film/substrate bilayers

Yanping Cao [1] and John W. Hutchinson [2] *

[1] AML, Department of Engineering Mechanics
Tsinghua University, 100084, Beijing, P. R. China
[2] School of Engineering and Applied Sciences
Harvard University, Cambridge, MA 02138 USA

Abstract

Wrinkling modes are determined for a two-layer system comprised of a neo-Hookean film bonded to an infinitely deep neo-Hookean substrate with the entire bilayer undergoing compression. The full range of the film/substrate modulus ratio is considered from the limit of a traction-free homogeneous substrate to very stiff films on compliant substrates. The role of substrate pre-stretch is considered wherein an unstretched film is bonded to a pre-stretched substrate with wrinkling arising as the stretch in the substrate is relaxed. An exact bifurcation analysis reveals the critical strain in the film at the onset of wrinkling. Numerical simulations carried out within a finite element framework uncover advanced post-bifurcation modes including period-doubling, folding and a newly identified mountain ridge mode.

Keywords: wrinkling, neo-Hookean bilayer, bifurcation, period-doubling, folding

This paper is dedicated to James R. Rice in celebration of his 70th birthday and his many extraordinary contributions to mechanics.

*Author for correspondence (hutchinson@husm.harvard.edu)

1. Introduction

A large literature exists reporting short wavelength buckling wrinkles of compressed thin films bonded to thick compliant substrates. Allen's [1] monograph on the mechanics of thin film wrinkling applies to structural systems where the surface film or layer is very stiff compared to the substrate. As applications of soft materials, such as elastomers and gels, grow, there is increasing interest in wrinkling of film/substrate bilayers where both materials are soft and the stiffness ratio of the film to the substrate is not necessarily very large [2]. An important limiting case is surface wrinkling of a compressed homogeneous substrate which Biot [3] analyzed for a neo-Hookean material.

In the first part of this paper, Biot's exact finite strain bifurcation analysis is extended to a bilayer system comprised of a neo-Hookean film bonded to an infinitely deep neo-Hookean substrate. Biot [3] considered several bilayer problems, but not the important case where the film and the substrate are jointly compressed, nor did he consider the role of substrate pre-stretch. Here, the critical bifurcation strain is obtained for the film/substrate modulus ratio ranging from the limit in which the film and substrate have the same modulus, i.e., a homogeneous substrate, to a very stiff film on a compliant substrate. The role of substrate pre-stretch is also considered. Substrate pre-stretching is a technique now widely used by experimentalist to produce compression in the film layer. A thin unstretched film is bonded to a thick pre-stretched substrate. Then, as the stretch in the substrate is relaxed, the film is compressed and wrinkling occurs. In the second part of the paper, numerical simulations are carried out in plane strain within a finite element framework to uncover advanced post-bifurcation modes including period-doubling, folding and a newly identified mountain ridge mode.

Both materials in the bilayer are incompressible neo-Hookean elastic materials. Quantitative details for other nonlinear elastic material models will differ somewhat from the results present in this paper. Nevertheless, the trends brought out for neo-Hookean materials are expected to have broad applicability. Moreover, when the film is very stiff compared to the substrate, the strain in the film remains small and, thus, it is expected that results in this range are applicable to any (incompressible) linear elastic film material. The ground state shear modulus of the film is μ_f and that of the substrate is μ_s. The thickness of the undeformed film is h; the substrate is infinitely deep.

Lagrangian coordinates, x_i $(i=1,3)$, specifying the locations of material points in the undeformed state of the film are identified in Fig. 1. The coordinate x_2 is perpendicular to the surface of the undeformed bilayer. The surface of the bilayer is traction-free. The stretches in the film and the substrate in the pre-bifurcation state are uniform and are denoted by $(\lambda_{1f}, \lambda_{2f}, \lambda_{3f})$ and $(\lambda_{1s}, \lambda_{2s}, \lambda_{3s})$, respectively. Pre-stretches in the substrate, if present, are denoted by $(\lambda_{1s}^0, \lambda_{2s}^0, \lambda_{3s}^0)$. Thus, with coordinates $(\overline{x}_1, \overline{x}_3)$ identifying material points in the interface of the undeformed substrate, the corresponding material points in the interface of the undeformed film to which they are attached are identified by $x_1 = \lambda_{1s}^0 \overline{x}_1$ and $x_3 = \lambda_{3s}^0 \overline{x}_3$. In the uniform pre-bifurcation state, the stretches in the film and substrate are related to one another by

$$\lambda_{1f} = \lambda_{1s} / \lambda_{1s}^0 \ , \ \lambda_{2f} = \lambda_{2s} / \lambda_{2s}^0 , \ \lambda_{3f} = \lambda_{3s} / \lambda_{3s}^0 \qquad (1)$$

For the combinations of compression and pre-stretch considered in this paper, the bifurcation mode is an incremental plane strain deformation in the (x_1, x_2) plane. In all cases, the normal deflection of the surface of the bifurcation mode is proportional to a sinusoidal variation of the form, $\cos(kx_1) = \cos(2\pi x_1 / \ell)$, where $\ell = 2\pi / k$ is the wrinkling wavelength referenced to the undeformed film and $\lambda_{1f}\ell$ is the wavelength in the deformed state.

2. Effect of substrate pre-stretch on wrinkling of stiff films on compliant substrates

Before considering the neo-Hookean bilayer, a result derived in the Appendix will be presented for wrinkling of a stiff linear elastic film on a compliant neo-Hookean substrate which has undergone a uniform pre-stretch, $(\lambda_{1s}^0, \lambda_{2s}^0, \lambda_{3s}^0)$, prior to attaching the film. The formulas below extend the well known result of Allen [1] by account for the fact that the incremental moduli of the pre-stretched neo-Hookean substrate change from the ground state and become anisotropic. In the extended result the film is isotropic and linearly elastic with modulus E_f and Poisson ratio ν_f. The formulas apply to arbitrary combinations of substrate pre-stretch and subsequent film compression under the assumption that the maximum compressive stress in the film is in the 1-direction

($\sigma_{11} = -\sigma$). The wrinkling mode is an incremental plane strain mode with normal surface deflection in the form $u_2 \propto \cos(k_0 x_1)$ with x_1 attached to material points in the undeformed film. The critical stress in the film and the associated wave number are

$$\frac{\sigma}{\bar{E}_f} = \frac{1}{4}\left(\Lambda \frac{3\mu_s}{\bar{\mu}_f}\right)^{2/3}, \quad k_0 h = \left(\Lambda \frac{3\mu_s}{\bar{\mu}_f}\right)^{1/3} \quad \text{with } \Lambda = \frac{1}{2\lambda_{3s}^0}\left(1+\lambda_{1s}^{0\,2}\lambda_{3s}^0\right) \tag{2}$$

Here, $\bar{E}_f = E_f/(1-\nu_f^2)$, $\mu_f = E_f/\left[2(1+\nu_f)\right]$ and $\bar{\mu}_f = \mu_f/\left[2(1-\nu_f)\right]$. The pre-stretch factor Λ is unity when there is no pre-stretch. This result was obtained in [4] for the special case of plane strain pre-stretch. This factor is for the neo-Hookean substrate. Nevertheless, the influence of pre-stretched predicted for this substrate are expected to be illustrative of other elastomeric materials that stiffen when stretched.

3. Bifurcation analysis of wrinkling of a bilayer of neo-Hookean materials

3.1 Plane strain compression with no substrate pre-stretch. With no pre-stretch in the substrate and the bilayer subject to plane strain compression, the pre-bifurcation stretches satisfy

$$\lambda_{3f} = \lambda_{3s} = 1, \ \lambda_{1f} = \lambda_{1s} \equiv \lambda_1, \ \lambda_{2f} = \lambda_{2s} \equiv \lambda_2 = 1/\lambda_1 \tag{3}$$

Compression in the 1-direction is considered with a (nominal) compressive strain defined by

$$\varepsilon = 1 - \lambda_1 \tag{4}$$

By dimensional arguments, the compressive strain at the wrinkling bifurcation, ε_W, is only a function of μ_f/μ_s. Details of the bifurcation analysis are given in the Appendix. The film and the substrate are each treated as a continuum with no approximation in the bifurcation analysis. The plot of ε_W as a function of μ_f/μ_s is given in Fig. 2. Included in Fig. 2 is the compressive bifurcation strain, ε_0, as predicted by (2) for plane strain:

$$\varepsilon_0 = \frac{1}{4}\left(\Lambda \frac{3\mu_s}{\mu_f}\right)^{2/3}, \quad k_0 h = \left(\Lambda \frac{3\mu_s}{\mu_f}\right)^{1/3} \quad \text{with } \Lambda = \frac{1}{2}\left(1+\lambda_{1s}^{0\,2}\right) \tag{5}$$

(with $\nu_f = 1/2$, $\bar{\mu}_f = \mu_f$ and $\varepsilon_0 = \sigma/\bar{E}_f$.) Remarkably, the simple formula (5) for ε_0 with $\Lambda = 1$, corresponding to Allen's result for an incompressible film and substrate with

no pre-stretch, retains reasonable accuracy even at modest ratios of the moduli with bifurcation strains that are not small. For this to be true, the strain in (5) must be interpreted as the nominal strain defined in (4).

The limit for the homogeneous case ($\mu_f / \mu_s = 1$) in Fig. 2 is $\varepsilon_W = 0.456$ corresponding to Biot's [3] result for surface wrinkling of a homogeneous neo-Hookean half space under plane strain compression. Because there is no length scale associated with the homogeneous half-space, the surface bifurcation mode in this limit can have any wavelength.[1] As recent work [6] has shown, surface wrinkling of a homogeneous half-space is highly unstable and imperfection-sensitive such that compressive strains as large as $\varepsilon_W = 0.456$ in the film are not likely to be achieved. Instead, finite strain creases in the film become energetically favorable when the compressive strain exceeds $\varepsilon = 0.35$ in plane strain compression [7,8]. Thus, one can anticipate that the bifurcation result in Fig. 2 for $\mu_f / \mu_s < 2$ is an upper bound in the sense that imperfections will trigger surface creases within the film before the wrinkling bifurcation mode can be attained. For larger μ_f / μ_s with smaller ε_W, the bifurcation mode has a unique wavelength proportional to the film thickness, h, as will be illustrated.

3.2 Plane strain compression with plane strain substrate pre-stretch. An undeformed film is attached to a substrate which has been subject to a pre-stretch, $\lambda_{1s}^0 > 1$, in plane strain with $\lambda_{3s}^0 = 1$ and $\lambda_{2s}^0 = 1/\lambda_{1s}^0$. The film/substrate system subsequently undergoes incremental plane strain compression with decreasing λ_{1s} subject to $\lambda_{3s} = 1$ and $\lambda_{2s} = 1/\lambda_{1s}$. The stretches in the film are given by (1). The effect of the pre-stretch on the critical compressive strain in the film, $\varepsilon_W = 1 - \lambda_{1f}$, at the onset of wrinkling is shown in Fig. 3. Included in this figure is the prediction of the simple

[1] In passing it is worth mentioning that surface wrinkling strain, $\varepsilon_W = 0.456$, is also the critical strain for wrinkling localized at the bonded interface between two semi-infinite half-spaces of neo-Hookean materials with different ground state moduli. This result, due to Biot [5], can be readily appreciated by noting that each half-space undergoes traction-free surface wrinkling at the same strain with arbitrary sinusoidal wavelength. Thus, the two wrinkled half-spaces can be "fit together" satisfying continuity of displacements and tractions.

formula (5) which becomes increasing accurate for $\mu_f / \mu_s \geq 10$. Pre-stretch has a large effect on the wrinkling strain when the film is stiff compared to the substrate such that, for increasing pre-stretch, ε_W scales with $\lambda_{1s}^{0\ 4/3}$.

Pre-stretch produces anisotropic stiffening of the substrate (see Appendix) which increases the wrinkling strain when the film is stiff compared to the substrate as seen in Fig. 3. In the range in which the ground state modulus of the film is only slightly larger than that of the substrate, the pre-stretch has the unexpected effect of lowering the critical bifurcation strain. This is seen in Fig. 4 where the critical bifurcation strain ε_W is plotted for the same levels of pre-stretch for a much smaller range of μ_f / μ_s. With $\mu_f / \mu_s = 1$ and no pre-stretch (i.e. an initially homogeneous substrate), $\varepsilon_W = 0.456$, corresponding to Biot's arbitrarily short wavelength surface mode as already noted. However, for all other combinations plotted in Fig. 4, the critical strain is below the Biot limit and the wavelength of the mode associated with the critical compressive strain has a wavelength that is long compared to the film thickness. Fig. 5 further highlights this unusual influence of substrate pre-stretch for the case in which the ground state modulus of the film and the substrate are the same ($\mu_f / \mu_s = 1$). In the range of pre-stretch, $1 < \lambda_{1s}^0 < 5$, the critical compressive strain in the film is less that the Biot strain and the wavelength of the critical mode is long compared to the film thickness. For pre-stretches greater than 5, the Biot mode again becomes critical. This behavior appears anomalous given the stiffening that occurs in the substrate under pre-stretch. However, as the substrate becomes anisotropic, some of the incremental moduli components diminish. In addition, as the film is compressed it's incremental in-plane stiffness increases. Evidently, the very different anisotropies that develop in the film and the substrate account for the behavior in Fig. 5, but a simple explanation of the anomaly is not apparent.

The dimensionless wave number, kh, of the mode from the exact analysis for the cases shown in Fig. 3 is plotted in Fig. 6. The normal deflection of the mode is proportional to $\cos(kx_1)$ where x_1 is defined in Section 1. The wavelength of the mode in the deformed state is $\ell = 2\pi\lambda_{1f} / k$. The plot for $\mu_f / \mu_s \geq 10$ includes the dimensionless wave number, $k_0 h$, from (5) which becomes increasing accurate for large

μ_f / μ_s. Pre-stretch also has an appreciable affect on the critical wave number such that it increases in proportion to $\lambda_{1s}^{0\ 2/3}$ when the pre-stretch is relatively large.

3.3 Uniaxial compression with uniaxial stressing pre-stretch. To illustrate the role of the deformation history on wrinkling, consider uniaxial pre-stretching followed by uniaxial compression, as is sometimes employed in wrinkling experiments. Specifically, consider pre-stretching of the substrate carried out under uniaxial tension such that $\lambda_{1s}^0 > 1$ with $\lambda_{2s}^0 = \lambda_{3s}^0 = 1/\sqrt{\lambda_{1s}^0}$. Then, the film is attached to the substrate and the substrate is assumed to undergo incremental uniaxial compressive stressing under decreasing λ_{1s} with $\lambda_{2s} = \lambda_{3s} = 1/\sqrt{\lambda_{1s}}$. Film stretches are given by (1). The compressive wrinkling strain in the film, $\varepsilon_W = 1 - \lambda_{1f}$, at bifurcation is plotted in Fig. 7. The corresponding predictions from (2) for this case are

$$\varepsilon_0 = \frac{1}{3}\left(\Lambda \frac{3\mu_s}{\mu_f}\right)^{2/3}, \quad k_0 h = \left(\Lambda \frac{3\mu_s}{\mu_f}\right)^{1/3} \quad \text{with } \Lambda = \frac{1}{2}\lambda_{1s}^{01/2}\left(1+\lambda_{1s}^{03/2}\right) \tag{6}$$

(now with $\nu_f = 1/2$, $\bar{\mu}_f = \mu_f$, $\varepsilon_0 = (4/3)\sigma / \bar{E}_f = \sigma / E_f$), and ε_0 is included in Fig.7. The trends are similar to those for plane strain deformations. For moderately large pre-stretch ε_W again scales with $\lambda_{1s}^{04/3}$.

The wrinkling strain of the homogeneous substrate is $\varepsilon_W = 0.556$ under uniaxial stressing conditions with no pre-stretch. Biot's [3] result for surface wrinkling bifurcation of a homogeneous neo-Hookean substrate under general uniform stretching is

$$\varepsilon_W = 1 - 0.5437/\sqrt{\lambda_3} \tag{7}$$

for conditions in which the maximum compressive stress acts in the 1-direction. This result provides the values quoted above for plane strain and uniaxial stressing. Under uniaxial stressing, substrate pre-stretch causes only a slight reduction of the critical strain in the domain of modulus ratios near unity (Fig. 7).

4. Numerical analysis of post-bifurcation modes under plane strain

A finite element model has been employed to investigate plane strain compression of the neo-Hookean bilayer at compressive strain levels well beyond the bifurcation strain. Advanced post-bifurcation modes are revealed for cases with and without substrate pre-stretch. Plane strain ($\lambda_{3f} = \lambda_{3s} = 1$) finite element simulations have been performed via the commercial software, ABAQUS [9]. The ratio of the anticipated wavelength to the element size is taken to be approximately 100. In the finite element simulations, the incompressible neo-Hookean material model is employed for both the film and the substrate. The hybrid element (CPE6MH in ABAQUS) suitable for simulations of incompressible materials is adopted. Two schemes are adopted to introduce initial stress-free geometric surface imperfections. For the case of no substrate pre-stretch, a linear perturbation procedure is accomplished using the "buckle" function in the software. The critical eigenmode scaled by a very small factor ($\cong 0.005h$) is introduced as a geometric imperfection into the mesh. For the case in which the substrate is pre-stretched, finite element simulations are first run by specifying a displacement $u_2 = 0.025h\cos(kx_1)$ at the upper surface, where k is the anticipated wave number. The computed displacement field is introduced as a stress-free geometric imperfection into the mesh.

In the post-buckling analysis, displacement-controlled loading is employed with u_1 (independent of x_2) and zero shear traction specified on the vertical sides of the model. The nominal compressive overall strain applied to the system after the film is attached to the substrate, ε, is defined exactly as in (4) in terms of the film stretch, λ_{1f}, evaluated in terms of the difference between u_1 on the two sides of the model. On the bottom surface, u_2 and the shear traction are taken to be zero. The width of the model is taken to be on the order of 5-10 wavelengths of the sinusoidal wrinkling mode, as will be evident from the deflection patterns. The depth of the substrate is taken to be more than 10 times the sinusoidal wavelength and, thus, sufficiently deep to ensure that there is no interaction with the modes and the bottom of the substrate—effectively, the substrate is infinitely deep. The numerical model relies on the slight initial geometric imperfection to initiate growth of the post-bifurcation modes.

It is not straightforward to simulate plane strain compression with substrate pre-stretch with the finite element software because of the necessity of specifying the mesh in advance. If a regular mesh is imposed on the bilayer followed by substrate pre-stretch, the film elements can be rendered inactive using the function, "model change, remove", but the resulting mesh in the film winds up highly distorted before the compression phase begins. This problem can be circumvented using features available in the software by the following steps. A background mesh is designed which shares nodes with the film mesh and which has a uniform ground state shear modulus. The entire film/substrate is then pre- stretched to the desired substrate pre-stretch. In this way, the mesh in the film deforms with the substrate. Before compression of both film and the substrate, the background mesh can be removed with the function, "model change, remove". Using the function, "model change, add", one can reactivate the film mesh, set the state of the film to be stress-free, and re-set the ground state modulus of the substrate to its correct value, μ_s. From this point, the system is subject to increments of plane strain compression.

4.1 Plane strain compression with no substrate pre-stretch. Numerical simulations have been performed for the bilayer modulus ratio in the range $3 \le \mu_f / \mu_s \le 80$ with results displayed in Fig. 8. The linear perturbation analysis using the "buckle" function in the software allows direct computation of ε_W, corresponding to the onset of the sinusoidal wrinkling mode. It is in good agreement with the result of Section 3.1.

Two very different post-bifurcation modes are observed depending on μ_f / μ_s. When μ_f / μ_s is large, the sinusoidal wrinkling mode is stable to strains that can be many times ε_W (see Fig. 9). Then, at a compressive strain denoted by ε_{PD} in Fig. 8, the sinusoidal mode transitions into a mode with twice the wavelength (see Fig. 9). This period-doubling mode would occur as a secondary bifurcation in a perfect system, but in the present simulations it is triggered by slight imperfections. The precise value of ε_{PD} is difficult to pin down in the simulations, as evident from the small variations in Fig. 8. For this bilayer system it is noted that $\varepsilon_{PD} \cong 0.2$ for all $\mu_f / \mu_s \ge 10$. For stiff films, the sinusoidal wrinkling mode is highly stable for relatively large compressions prior to the

onset of period-doubling, as illustrated in Fig. 9. A combined analytical-experimental study [10] of the nonlinear evolution of the sinusoidal wrinkling mode prior to period-doubling has been carried for stiff films on compliant neo-Hookean substrates. Studies of period-doubling for stiff thin films on compliant elastomer substrates, including experimental realizations of the mode, have been presented in [4] and [11]. In addition, period-doubling in wrinkling has been also been identified in the system of a cylindrical cavity covered by a stiff surface layer [12].

For $\mu_f / \mu_s < 10$, the post-bifurcation mode changes to what will be called a "folding mode" at a strain denoted by, ε_F, that is only slightly above ε_W, as seen in Fig. 8. The steps involved in the formation of the folding mode are illustrated by the example in Fig. 10. A localization develops within the multiple undulations of the sinusoidal mode where, in the example in Fig. 10, two neighboring undulations grow relative to all the others—a distinct two-lobed undulation develops. With a slight further increase of overall compression, the localization process continues as one of the two undulations becomes dominant in the form of an incipient fold. Then, at the deepest point on this incipient fold, a crease is nucleated at the film surface. The simulation is terminated at this point. The localized folding mode was observed in all the simulations performed in the range $3 \le \mu_f / \mu_s < 10$.

4.2 Plane strain compression with modest substrate pre-stretch, $\lambda_{1s}^0 = 1.3$. When the substrate pre-stretch is relatively small as in Fig. 11, the behavior is qualitatively similar to that just described for the case on no pre-stretch. The pre-stretch shifts the transition from folding to period-doubling to somewhat larger μ_f / μ_S and, more significantly, it delays the onset of the double-period mode to larger strains. An example of evolution of the sinusoidal mode to the period-doubling mode for $\mu_f / \mu_S = 186$ is given in Fig. 12.

4.3 Plane strain compression with "large" substrate pre-stretch, $\lambda_{1s}^0 = 2$. The behavior described above changes dramatically for a larger pre-stretch, $\lambda_{1s}^0 = 2$. In this case, an entirely different mode is observed at compressive strains in the film that are

only modestly larger than the bifurcation strain, ε_W, as seen in Figs. 13 and 14. For the entire range of modulus ratio for which the simulations have been performed, $4 \le \mu_f / \mu_S \le 1000$, the secondary mode observed is the "mountain ridge mode", labeled so for reasons that will be evident from the mode shape in Fig. 14. Like the folding mode, this mode is a compressive localization. As the ridge forms, it relaxes the compression in the film on both sides of itself and thereby reduces the amplitudes of the wrinkles in its neighborhood. Similar stress relaxation is seen for on either side of a buckle delamination when the film is sufficiently stiff compared to the substrate [13]. As seen in Fig. 14, further overall compression causes more mountain ridges to form. For stiff films ($\mu_f / \mu_S = 836$ in Fig. 14), the overall compressive strains at which the mountain ridges form are not nearly as large as the strains required for period-doubling seen in Figs. 8 and 11 for the other cases. Thus, this phenomenon should be expected for any linear elastic film material.

5. Conclusions

The neo-Hookean film/substrate bilayer admits a rich variety of wrinkling modes, especially when pre-stretch of the substrate is considered. In all cases, the first mode to appear as the bilayer is compressed is the sinusoidal wrinkling mode associated with bifurcation from the bi-uniform state. The compressive strain in the film at bifurcation, ε_W, depends on the substrate pre-stretch, λ_{1s}^0, as well as the ground state modulus ratio, μ_f / μ_S. For systems with a modest stiffness difference between the film and substrate (e.g., $1 < \mu_f / \mu_S < 10$), the bifurcation strain is relatively large and no doubt strongly dependent on the fact that the film has been taken to be a neo-Hookean material. For stiffer films, the bifurcation strain is relatively small such that it and its associated mode should be applicable to any linear elastic film material. When the film is stiff (i.e., $\mu_f / \mu_S \ge 100$), the simple formula (2) generalizes the well known formula of Allen [1] to account for the fact that the incremental moduli of the pre-stretched substrate are different from its ground state moduli. This formula applies specifically to neo-Hookean

substrates but is expected to reflect the role of pre-stretch for any elastomeric material that stiffens as it is stretched.

The second mode to appear as the system is compressed beyond bifurcation can be one of several advanced post-bifurcation modes, including folding, period-doubling and mountain ridging. Folding and mountain ridging involve a localization process in which the local deflection of the film relaxes compression in its neighborhood thereby growing at the expense of the undulations in its neighborhood. Which one of the advanced mode to appear depends on the combination of the ground state modulus ratio, μ_f / μ_S, and substrate pre-stretch, λ_{1s}^0. The set of numerical simulations presented here have been limited to two levels of pre-stretch, although a selected number of additional simulations at other pre-stretches indicate that the modes reported in Section 4 are not isolated events. It remains for further work to perform a more exhaustive set of simulations that would map the occurrence of the advanced modes as a function of ground state modulus ratio, substrate pre-stretch and overall compression. Pre-stretch induces anisotropic incremental moduli in the substrate, increasing some components and decreasing others. The anisotropic moduli play an important role in selecting the advanced mode, and these moduli depend on the constitutive model of the substrate. Thus, to an extent which is not yet established, the occurrence of the various advanced modes revealed here may differ for other substrate constitutive models.

To our knowledge, there have been no reported experimental observations of the mountain ridge mode in the literature related to stiff films on compliant elastomer substrates, but it is possible that experiments have not yet been performed in the relevant range of pre-stretch. The mountain ridge mode occurs at relative small compressive strains for stiff films. Thus, it should be realizable for any linear elastic film material on a substrate can be reasonably approximated as a neo-Hookean material.

Appendix

Bifurcation analysis of neo-Hookean bilayer. The equations governing the bifurcation problem are constructed from exact solutions for increments of displacements and stresses in a uniformly stretched layer. Let λ_i, $i = 1,3$ be the uniform stretches with

$\lambda_1\lambda_2\lambda_3 = 1$ and $r = \lambda_2 / \lambda_1$. In a finite thickness neo-Hookean layer with ground state shear modulus μ, separated solutions to the field equations for the incremental problem exist with displacement increments, $(u_1, u_2) = (U_1 \sin(kx_1), U_2 \cos(kx_1))$, given by

$$\begin{aligned} U_1 &= -c_1 e^{rkx_2} - c_2 r^{-1} e^{kx_2} + c_3 e^{-rkx_2} + c_4 r^{-1} e^{-kx_2} \\ U_2 &= c_1 e^{rkx_2} + c_2 e^{kx_2} + c_3 e^{-rkx_2} + c_4 e^{-kx_2} \end{aligned} \tag{8}$$

assuming $r \neq 1$. This representation is degenerate for $r = 1$, but the solution for this limit is not required here. Note that the current stretch state enters (8) only through r. The solution holds for any k. The Cartesian coordinates (x_1, x_2) label material points in the undeformed layer and the displacement increments are with respect to this coordinate system. Nominal stress increments, $(n_{21}, n_{22}) = (N_{21} \sin(kx_1), N_{22} \cos(kx_1))$, with components referred to the same coordinate system and defined as force per undeformed area, are given by

$$\begin{aligned} N_{21} &= -\mu k \left[c_1 2re^{rkx_2} + c_2 r^{-1}(r^2+1) e^{kx_2} + c_3 2re^{-rkx_2} + c_4 r^{-1}(r^2+1) e^{-kx_2} \right] \\ N_{22} &= -\mu k \left[-c_1 r^{-1}(r^2+1) e^{rkx_2} - c_2 2e^{kx_2} + c_3 r^{-1}(r^2+1) e^{-rkx_2} + c_4 2e^{-kx_2} \right] \end{aligned} \tag{9}$$

This Lagrangian formulation, which employs the components of the second Piola-Kirchhoff stress, is the same used in the study of the stability of wrinkling of a homogeneous half-space [6]. The reader is referred to [6] or to Biot's book [5] for background details.

For the film layer, with $0 \le x_2 \le h$, $\mu = \mu_f$ and $r = r_f = \lambda_{2f} / \lambda_{1f}$, enforce $(N_{21}, N_{22}) = 0$ on $x_2 = h$ to obtain (c_3, c_4) in terms of (c_1, c_2):

$$\begin{bmatrix} c_3 \\ c_4 \end{bmatrix} = A \begin{bmatrix} c_1 \\ c_2 \end{bmatrix} \tag{10}$$

$$\text{with} \quad A = \begin{bmatrix} 2re^{-rkh} & r^{-1}(r^2+1)e^{-kh} \\ r^{-1}(r^2+1)e^{-rkh} & 2e^{-kh} \end{bmatrix}^{-1} \begin{bmatrix} -2re^{rkh} & -r^{-1}(r^2+1)e^{kh} \\ r^{-1}(r^2+1)e^{rkh} & 2e^{kh} \end{bmatrix}$$

Then solve for (N_{21}, N_{22}) on $x_2 = 0^+$ in terms of (c_1, c_2):

$$\begin{bmatrix} N_{21} \\ N_{22} \end{bmatrix} = \mu_f kB \begin{bmatrix} c_1 \\ c_2 \end{bmatrix} \tag{11}$$

$$\text{with } B = \begin{bmatrix} -2r(1+A_{11}) - r^{-1}(r^2+1)A_{21} & -r^{-1}(r^2+1)(1+A_{22}) - 2rA_{12} \\ r^{-1}(r^2+1)(1-A_{11}) - 2A_{21} & 2(1-A_{22}) - r^{-1}(r^2+1)A_{12} \end{bmatrix}$$

Next, solve for (U_1, U_2) on $x_2 = 0^+$ in terms of (c_1, c_2) using (8) and (10):

$$\begin{bmatrix} U_1 \\ U_2 \end{bmatrix} = C \begin{bmatrix} c_1 \\ c_2 \end{bmatrix} \quad \text{with } C = \begin{bmatrix} -1 + A_{11} + r^{-1}A_{21} & -r^{-1} + A_{12} + r^{-1}A_{22} \\ 1 + A_{11} + A_{21} & 1 + A_{12} + A_{22} \end{bmatrix} \tag{12}$$

By (11) and (12), the increments of nominal stress and displacement on the bottom of the film layer having a traction-free top surface are related by

$$\begin{bmatrix} N_{21} \\ N_{22} \end{bmatrix} = \mu_f kBC^{-1} \begin{bmatrix} U_1 \\ U_2 \end{bmatrix} \text{ on } x_2 = 0^+ \tag{13}$$

Now consider the semi-infinite substrate. If the substrate has a pre-stretch, λ_{1s}^0, relative to the film, the coordinate in the substrate relative to its undeformed state is $\bar{x}_1 = x_1 / \lambda_{1s}^0$. Continuity of increments of traction and displacement across the interface require

$$\frac{1}{\lambda_{1s}\lambda_{3s}} \left(N_{21}\sin(\bar{k}\bar{x}_1), N_{22}\cos(\bar{k}\bar{x}_1) \right)^- = \frac{1}{\lambda_{1f}\lambda_{3f}} \left(N_{21}\sin(kx_1), N_{22}\cos(kx_1) \right)^+ \tag{14}$$

$$\left(U_1\sin(\bar{k}\bar{x}_1), U_2\cos(\bar{k}\bar{x}_1) \right)^- = \left(U_1\sin(kx_1), U_2\cos(kx_1) \right)^+ \tag{15}$$

One condition is $\bar{k}\bar{x}_1 = kx_1$ and, thus, $\bar{k} = \lambda_{1s}^0 k$. The factors, $1/\lambda_1\lambda_3$, multiplying the increments in (14) account for the fact that the nominal stress increments in the two layers are defined relative to different undeformed areas if the substrate has a pre-stretch.

The separated solution (8) applies to the semi-infinite substrate with $\mu = \mu_s$ $r = r_s = \lambda_{2s} / \lambda_{1s}$, $k \to \bar{k}$ and $c_3 = c_4 = 0$. It is straightforward to show that the relation between (N_{21}, N_{22}) and (U_1, U_2) on the top of the substrate ($x_2 = 0^-$) is

$$\begin{bmatrix} N_{21} \\ N_{22} \end{bmatrix} = \mu_S \bar{k} D \begin{bmatrix} U_1 \\ U_2 \end{bmatrix} \quad \text{with} \quad D = \begin{bmatrix} r_s + 1 & -(r_s - 1) \\ -(r_s - 1) & r_s^{-1}(r_s + 1) \end{bmatrix} \tag{16}$$

The last step is to enforce continuity of traction and displacement increments across the interface, (14) and (15), using (13), (16) and (1); this requires

$(U_1, U_2)^+ = (U_1, U_2)^- \equiv (U_1, U_2)$ and

$$E\begin{bmatrix} U_1 \\ U_2 \end{bmatrix} = 0 \quad \text{with} \quad E = BC^{-1} - \frac{1}{\lambda_{3s}^0}\frac{\mu_s}{\mu_f} D \tag{17}$$

The eigenvalue problem governing bifurcation is $|E| = 0$. The eigenvalue associated with the critical compressive strain must be minimized over all values of kh. The solution to the eigenvalue problem is carried out numerically.

Effect of substrate pre-stretch on wrinkling bifurcation of stiff films. The extension (2) of Allen's result [1] employs the relation (16) between the increments of traction and displacement as the elastic foundation onto which a compressed thin stiff plate is attached. With incremental normal and tangential displacements to the plate/substrate interface given by $(u_1, u_2) = (U_1 \sin(k_0 x), U_2 \cos(k_0 x))$, the resisting traction increments of the foundation are $(t_1, t_2) = (T_1 \sin(k_0 x), T_2 \cos(k_0 x))$ where, by (16),

$$\begin{bmatrix} T_1 \\ T_2 \end{bmatrix} = \frac{\mu_S k_0}{\lambda_{3s}^0} D \begin{bmatrix} U_1 \\ U_2 \end{bmatrix} \tag{18}$$

Here, the traction increments have been transformed to force per unit area of the plate in the current compressed state; D is given in (16) with $r_s = \lambda_{2s}^0 / \lambda_{1s}^0$. The separated equations governing the incremental deformation of the compressed plate are

$$\begin{aligned} &\bar{E}_f h k_0^{\,2} U_1 = -T_1 \\ &\left((\bar{E}_f h^3/12) k_0^{\,4} - \sigma h k_0^{\,2}\right) U_2 = -T_2 + \alpha T_1 k_0 h/2 \end{aligned} \tag{19}$$

where $\bar{E}_f = E_f/(1-\nu_f^{\,2})$, σ is the compressive stress in the plate, h is its thickness, and $\alpha = 1$ with the interface at the bottom of the plate and $\alpha = 0$ if one imagines (as an approximation) that the mid-surface of the plate is attached to the top of the substrate. Here, we will be content in using the same approximations implicit in Allen's analysis by ignoring the coupling between the two equations in (19), i.e., by focusing on the second equation with $\alpha = 0$ and neglecting the contribution of U_1. The result after minimizing σ with respect to k_0 is (2). The fully coupled equations (19) with $\alpha = 1$ can be used to generate more accurate predictions than the extension in (2), as illustrated in [14] for the case of no substrate pre-stretch.

Acknowledgment YPC acknowledges the financial support from Tsinghua University (2009THZ02122).

References

[1] Allen, H. G., 1969, *Analysis and design of sandwich panels*, Pergamon Press, New York.

[2] Multiple authors, 2010, "Theme issue: The physics of buckling", Soft Matter **6**.

[3] Biot, M.A., 1963, "Surface instability of rubber in compression", Appl. Sci. Res. **12**, 168-182.

[4] Sun, J-Y., Xia, S., Moon, M-Y., Oh, K.H., and Kim, K-S., 2010, "Folding wrinkles of a thin stiff layer on a soft substrate", Proc. Roy. Soc. A. doi 10.1098/rspa.2011.0567.

[5] Biot, M.A., 1965, *Mechanics of incremental deformation.* New York, US, Wiley.

[6] Cao, Y., and Hutchinson, J. W., 2012, "From wrinkles to creases in elastomers: the instability and imperfection-sensitivity of wrinkling", Proc. Roy. Soc. A. **468**, 94-115.

[7] Holfeld, E.B., and Mahadevan, L., 2011, "Unfolding the sulcus", Phys. Rev. Letters **106**, 105702-1-4.

[8] Hong, W., Zhao, X., and Suo, Z., 2009, "Formation of creases on the surfaces of elastomers and gels", App. Phys. Letters **95**, 111901-1-3.

[9] ABAQUS analysis user's manual, version 6.8, (2008).

[10] Song, J., Jiang, H., Liu, Z.J., Khang, D.Y., Huang, Y., Rogers, J.A., Lu, C., and Koh, C.G., 2008, "Buckling of a stiff thin film on a compliant substrate in large deformation", Int. J. Solids Structures **45**, 3107-3121.

[11] Brau, F., Vandeparre, H., Sabbah, A., Poulard, C., Boudaoud, A., and Damman, P., 2010, "Multiple-length-scale elastic instability mimics parametric resonance of nonlinear oscillators", Nature Materials **7**, 56-60.

[12] Li, B., Cao, Y. P., Feng, X. Q., and Gao, H. J., 2011, "Surface wrinkling of mucosa induced by volumetric growth: Theory, simulation and experiment", J. Mech. Phys. Solids **59**, 758-774.

[13] Mei, H., Landes, C. M., and Huang, R., 2011, "Concomitant wrinkling and buckle-delamination of elastic thin films on compliant substrates", Mechanics of Materials **43**, 627-642.

[14] Cai, S., Breid, D., Crosby, A.I., Suo, Z., and Hutchinson, J.W., 2011, "Periodic patterns and energy states of buckled films on compliant substrates", J. Mech. Phys. Solids **59**, 1094-1114.

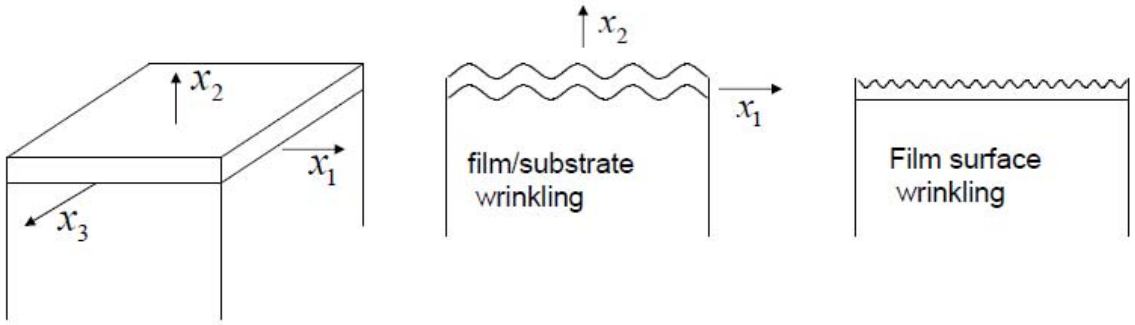

Fig. 1 Geometry of the film/substrate system and illustrations of wrinkling modes involving interaction between the film and substrate and a shallow surface mode. The cases considered in this paper all correspond to incremental plane strain bifurcations in the (x_1, x_2) plane.

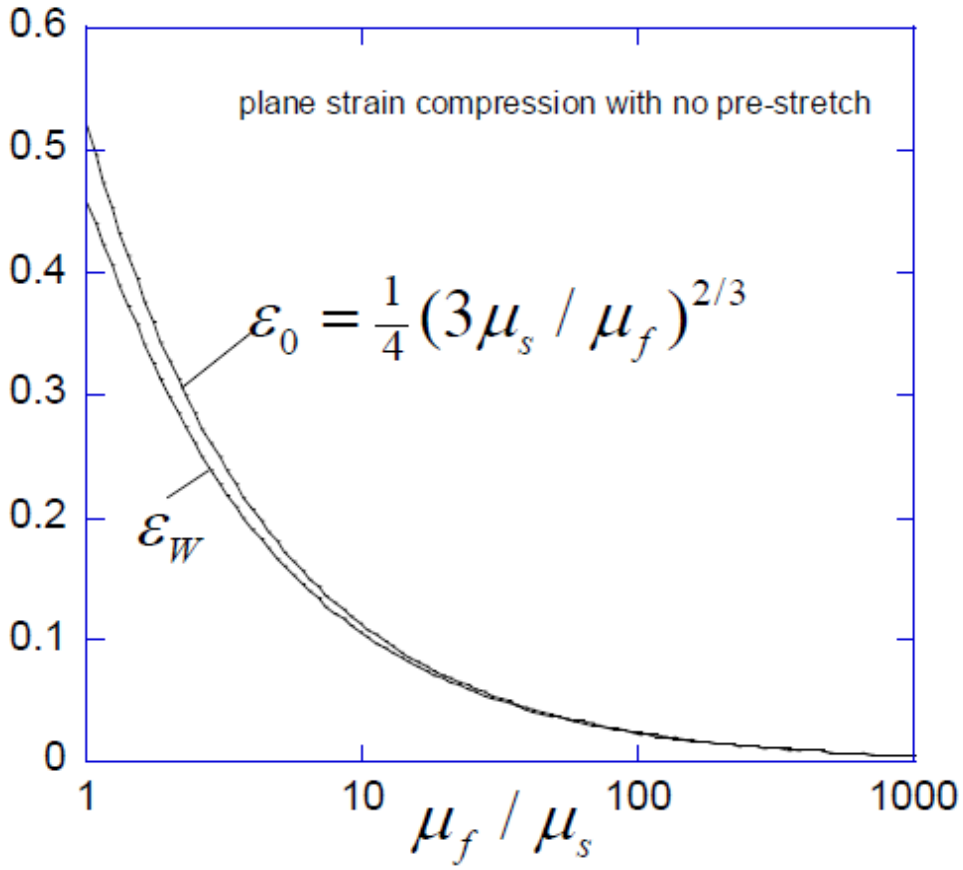

Fig. 2 Compressive strain in the film at wrinkling, ε_W, as a function of the film/substrate modulus ratio of the two neo-Hookean materials for plane strain compression with no substrate pre-stretch. The prediction, ε_0, of the simple formula (5) for wrinkling of a stiff linear elastic film on a compliant linear substrate is also shown.

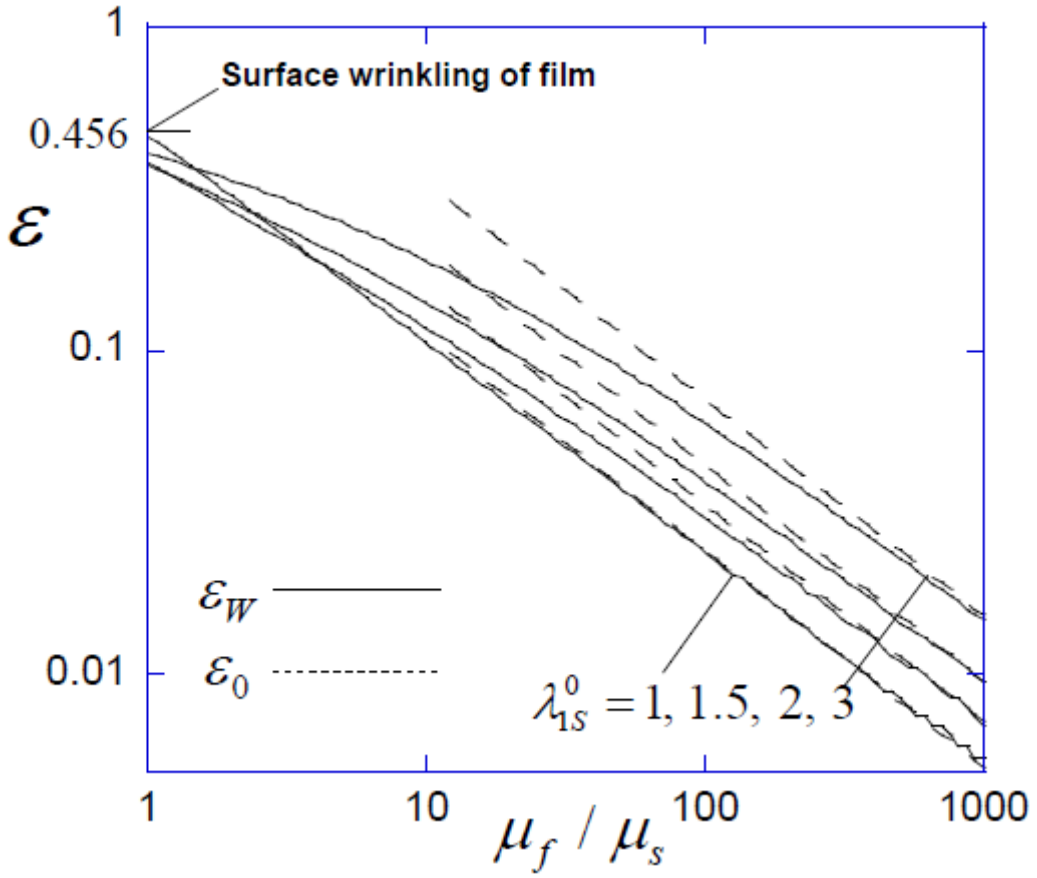

Fig. 3 Compressive strain in the film at wrinkling, ε_W, as a function of the film/substrate modulus ratio of the two neo-Hookean materials for plane strain compression showing the influence of plane strain substrate pre-stretch, λ_{1s}^0. The prediction, ε_0, of the simple formula (5) for wrinkling of a stiff linear elastic film on a compliant pre-stretched substrate is also shown. The range $1 \le \mu_f / \mu_s \le 5$ is magnified in Fig. 4.

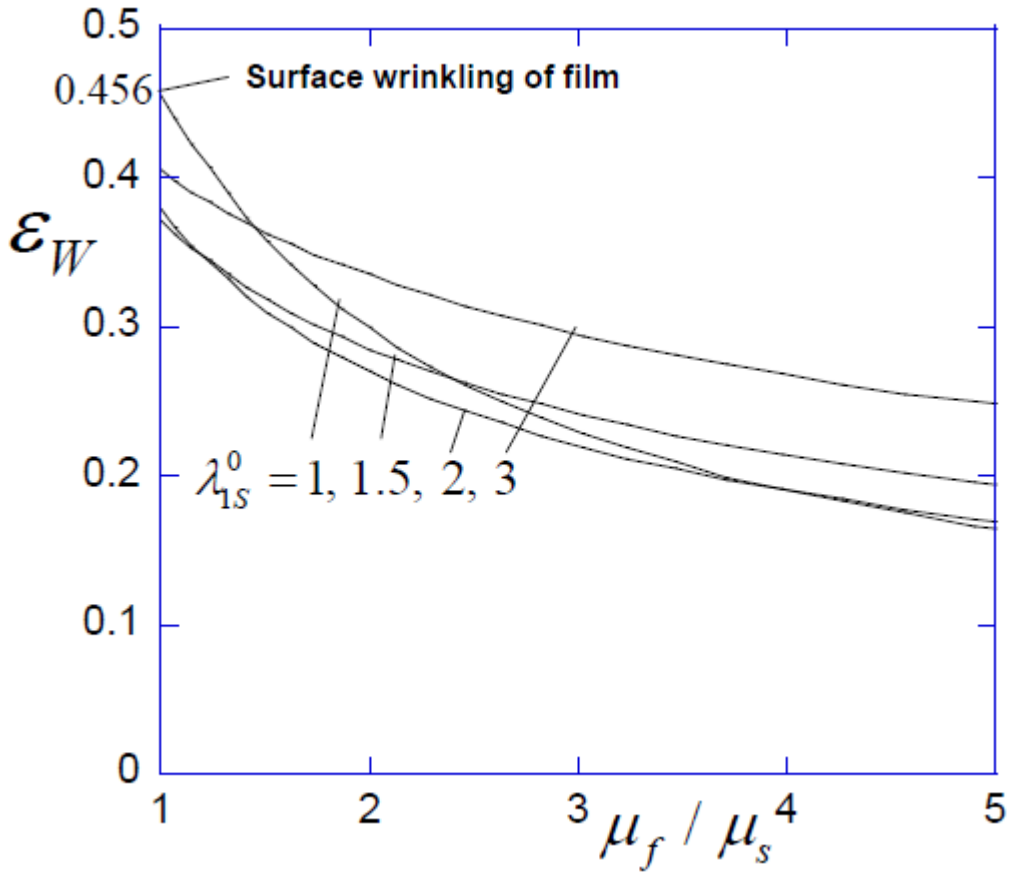

Fig. 4 Compressive strain in the film at wrinkling, ε_W, as a function of the film/substrate modulus ratio of the two neo-Hookean materials for plane strain compression showing the influence of plane strain substrate pre-stretch, λ_{1s}^0, in the range in which the ratio of the film to substrate modulus is not large.

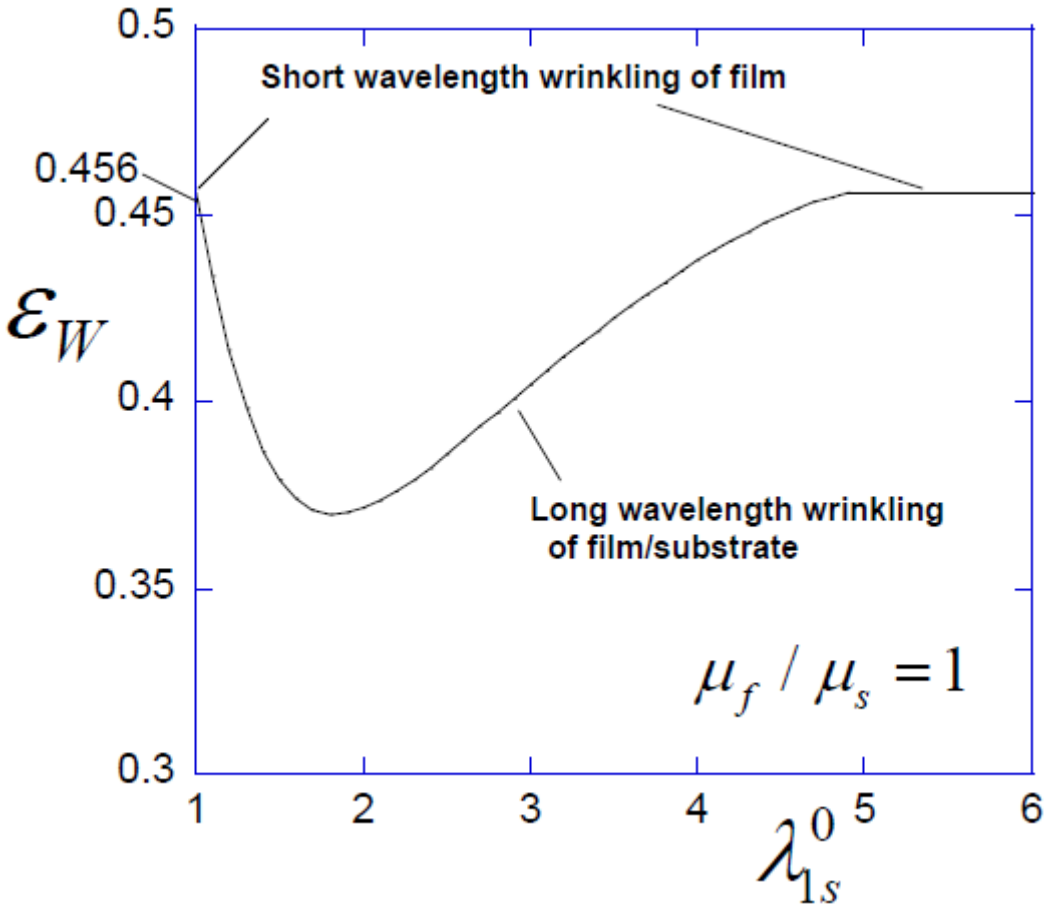

Fig. 5 Compressive strain in the film at wrinkling, ε_W, for plane strain compression showing the influence of plane strain substrate pre-stretch, λ_{1s}^0, for neo-Hookean films and substrates that have the same ground state modulus ($\mu_f / \mu_s = 1$). In the range of pre-stretch, $1 < \lambda_{1s}^0 < 5$, the critical mode is not the short wavelength surface mode but rather a mode with wavelength that is long compared to film thickness.

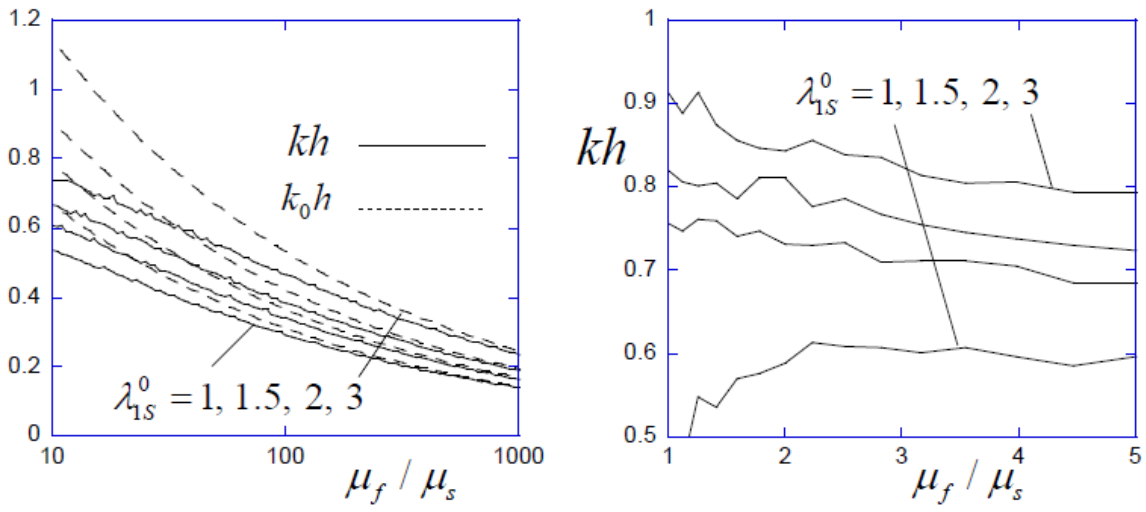

Fig. 6 Dimensionless wave number of the wrinkling mode as a function of the film/substrate modulus ratio of the two neo-Hookean materials for plane strain compression including the influence of plane strain substrate pre-stretch. The prediction, $k_0 h$, from the simple formula (5) for wrinkling of a stiff linear elastic film on a compliant pre-stretched substrate is also shown in the range of large stiffness ratio. The normal deflection of the top surface of the film has the form $u_2 \propto \cos(kx_1)$ where x_1 identifies material point locations in the undeformed film. Other than the limit for $\mu_f / \mu_s = 1$ with $\lambda_{1s}^0 = 1$ which is not plotted, the critical mode has a wavelength that is large compared to the film thickness.

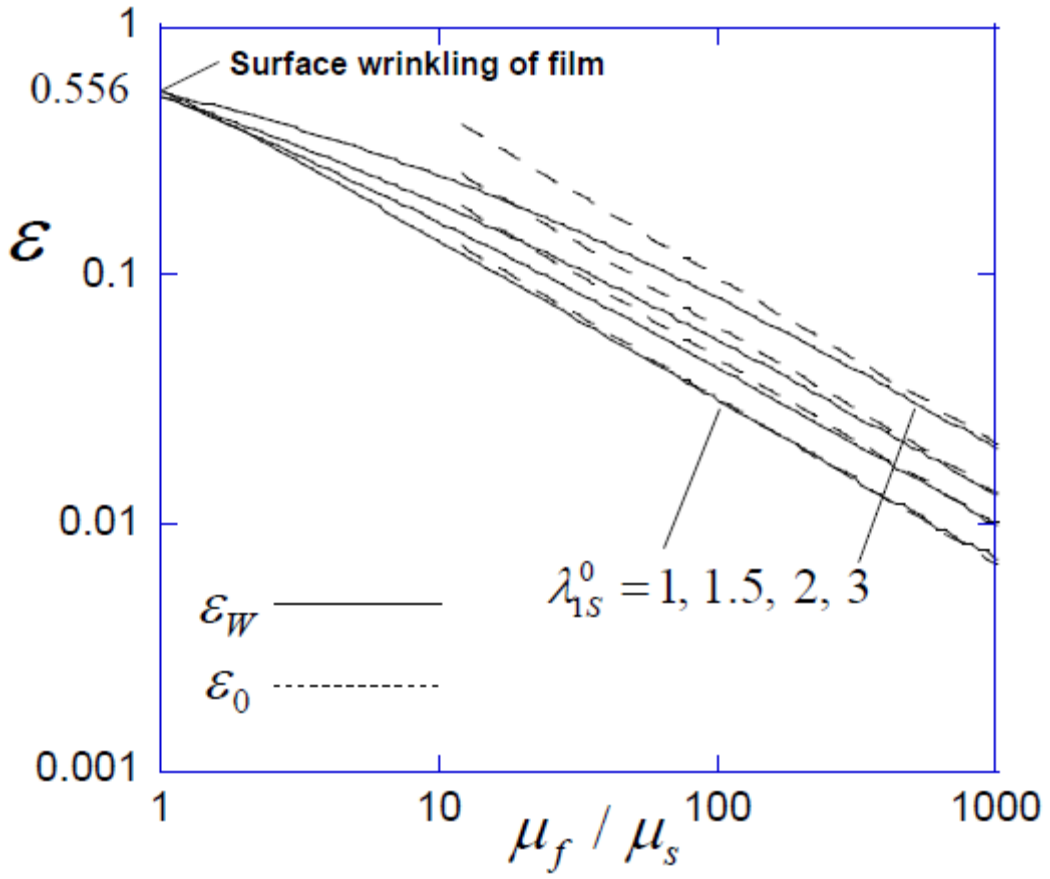

Fig. 7 Compressive strain in the film at wrinkling, ε_w, as a function of the film/substrate modulus ratio of the two neo-Hookean materials for uniaxial compression showing the influence of substrate pre-stretch under uniaxial tension. The prediction, ε_0, of the simple formula (6) for wrinkling of a stiff linear elastic film on a compliant pre-stretched substrate is also shown.

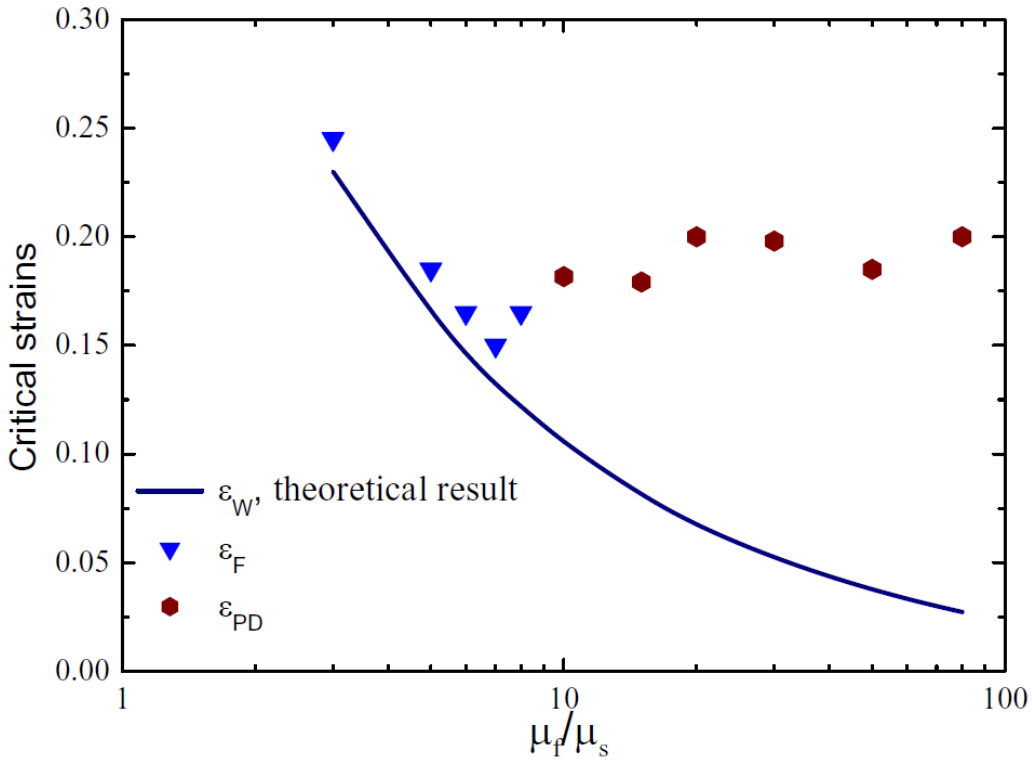

Fig. 8 Post-bifurcation behavior in the neo-Hookean bilayer under plane strain compression with no substrate pre-stretch computed using the finite element model. The critical compressive strain at the onset of wrinkling, ε_W, is the theoretical result of Section 3.1. The compressive strain at the onset of two distinct post-bifurcation modes is also indicated. For $\mu_f / \mu_s \geq 10$, period-doubling (see Fig. 9) is the first post-bifurcation mode encountered at strain ε_{PD}. For $\mu_f / \mu_s < 10$, the post-bifurcation mode is a fold that occurs at a strain denoted by ε_F that is only slightly greater than ε_W. It subsequently develops a local crease (see Fig. 10)

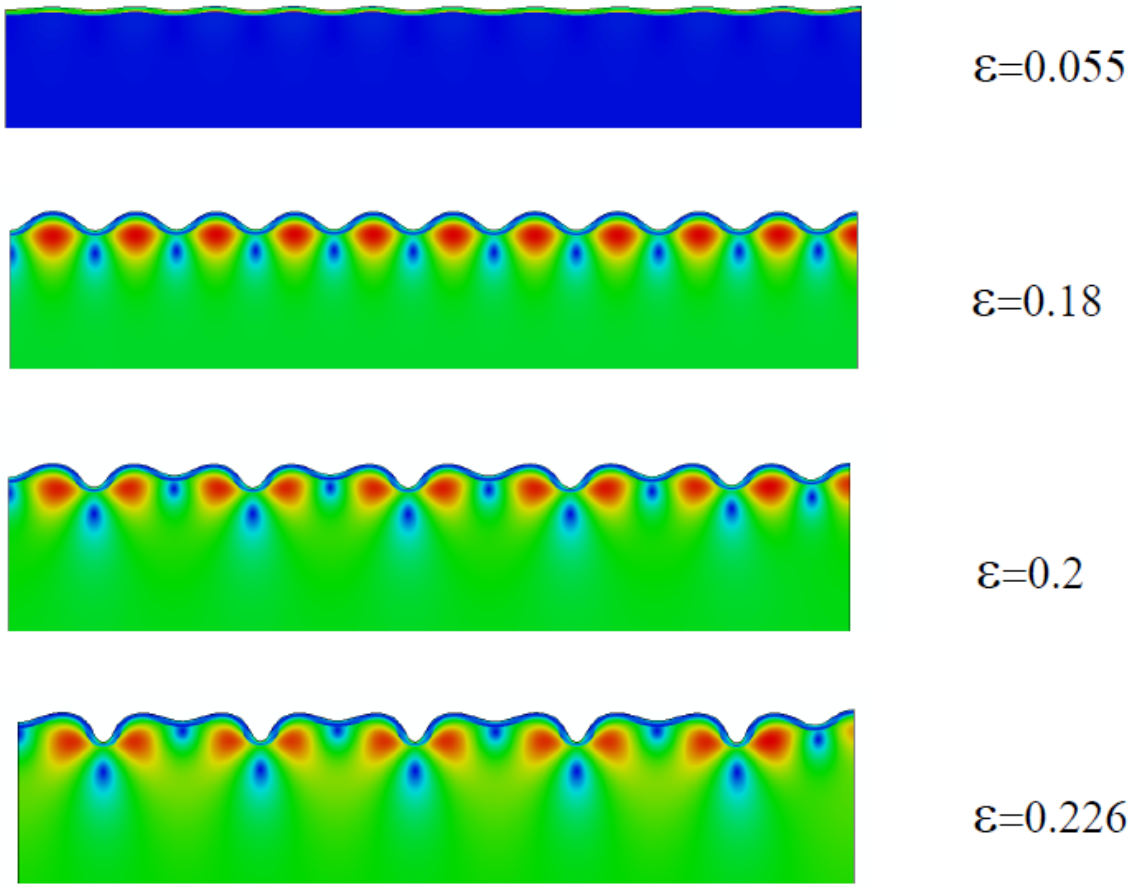

Fig. 9 Plane strain compression with $\mu_f / \mu_s = 30$ and no substrate pre-stretch. Bifurcation first occurs as a sinusoidal wrinkling mode ($\varepsilon \cong 0.055$). The sinusiodal mode is stable to much larger strains (e.g. $\varepsilon = 0.18$). At a compressive strain of approximately $\varepsilon = 0.2$ a secondary bifurcation occurs corresponding to the onset of period doubling. With a slight further increase of compression to $\varepsilon = 0.226$ the period-doubling mode is firmly established. This behavior is representative of bilayers with $\mu_f / \mu_s > 10$ if there is no pre-stretch.

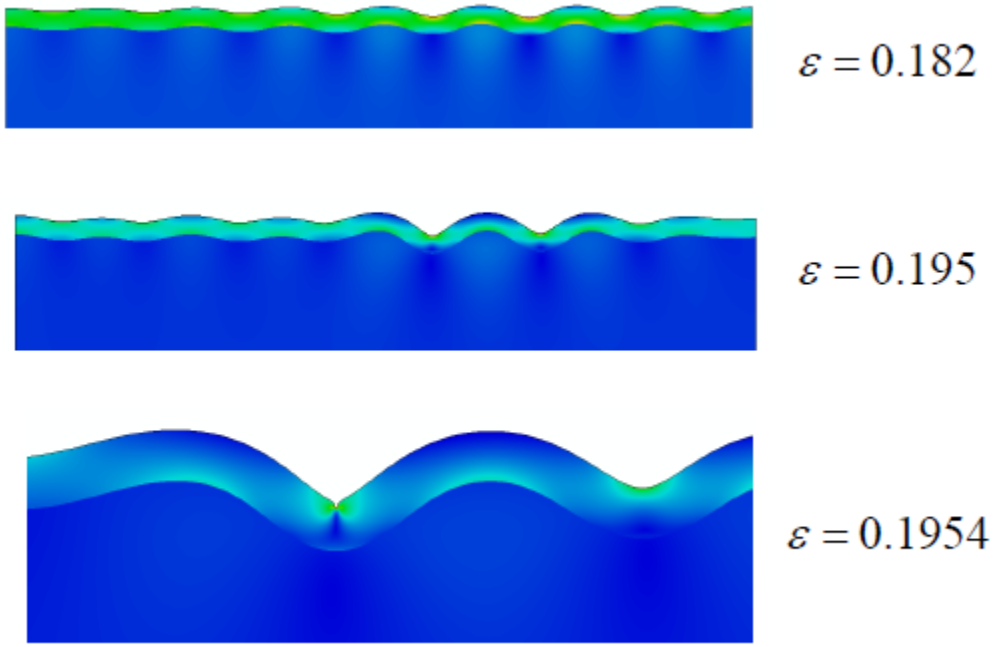

Fig. 10 Plane strain compression with $\mu_f / \mu_s = 5$ and no substrate pre-stretch. Bifurcation into the sinusoidal wrinkling mode occurs at $\varepsilon \cong 0.175$. Already at a strain slightly above the onset of bifurcation ($\varepsilon = 0.182$) the deflection is showing signs that it is evolving away from the sinusoidal mode. At $\varepsilon = 0.195$ the film deflection has localized into two side-by-side incipient folds. With a slight additional increase in strain ($\varepsilon = 0.1954$) the fold on the left becomes dominant and a crease has begun to form in the film at the point of maximum local compression. This behavior is representative of bilayers with $\mu_f / \mu_s < 10$ and no pre-stretch.

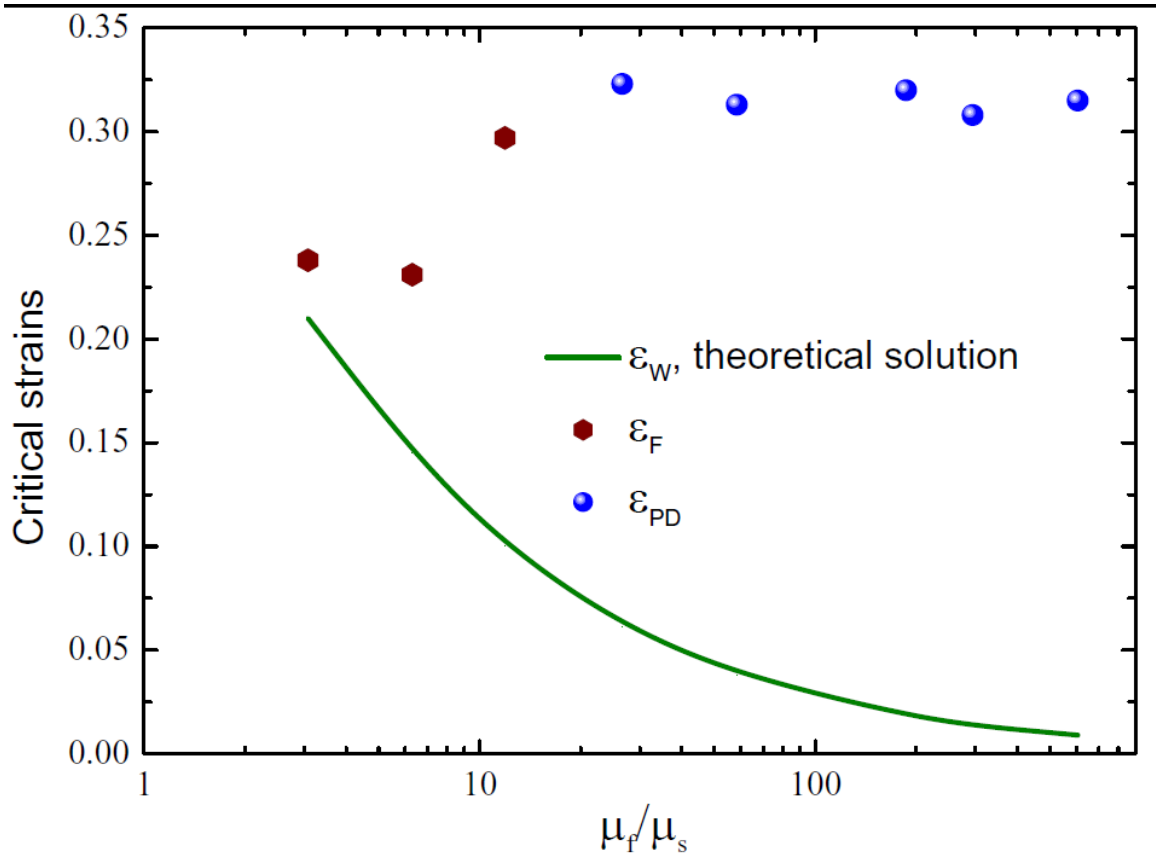

Fig. 11 Numerical simulations of the post-bifurcation modes for plane strain compression with a relatively small plane strain pre-stretch of the substrate, $\lambda_{1s}^{0}=1.3$. The curve for the bifurcation strain, ε_W, at the onset of sinusoidal wrinkling is that from the theoretical calculation in Section 3.2. The post-bifurcation behavior with small pre-stretch is qualitatively similar to the case with no pre-stretch, although the secondary modes are delayed to larger overall compressive strains. Period-doubling occurs when $\mu_f / \mu_s \geq 20$ (see Fig. 12) with folding at smaller values of the modulus ratio.

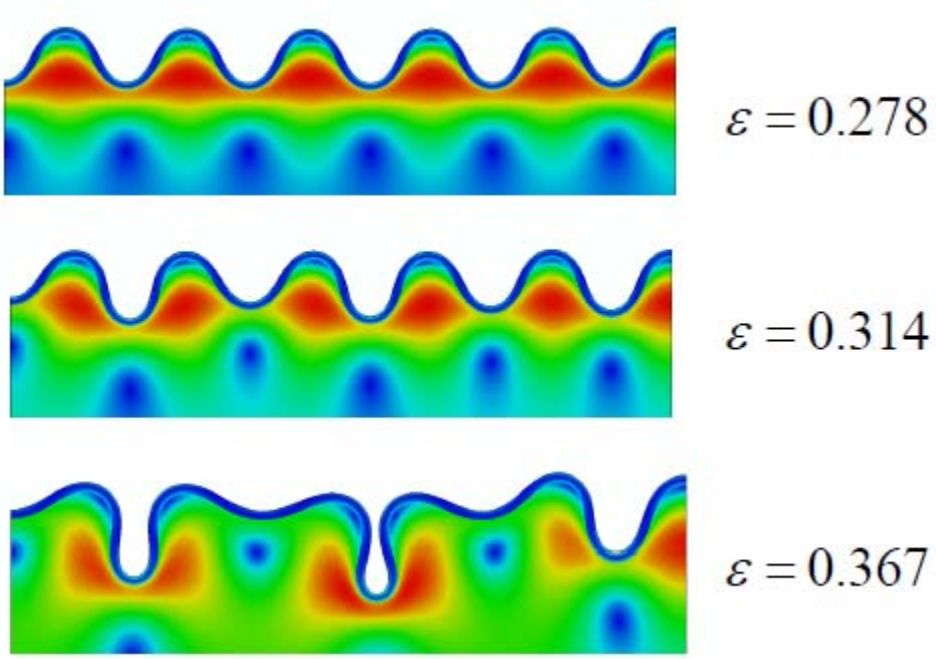

Fig. 12 Evolution of wrinkling mode under plane strain compression with a plane strain substrate pre-stretch $\lambda_{1s}^{0} = 1.3$ for $\mu_f / \mu_S = 186$. The sinusoidal wrinkling mode associated with bifurcation at $\varepsilon_W = 0.019$ is stable to much larger strains (e.g., $\varepsilon = 0.278$ above). The onset of period-doubling is evident at $\varepsilon = 0.314$ and is fully developed at $\varepsilon = 0.367$.

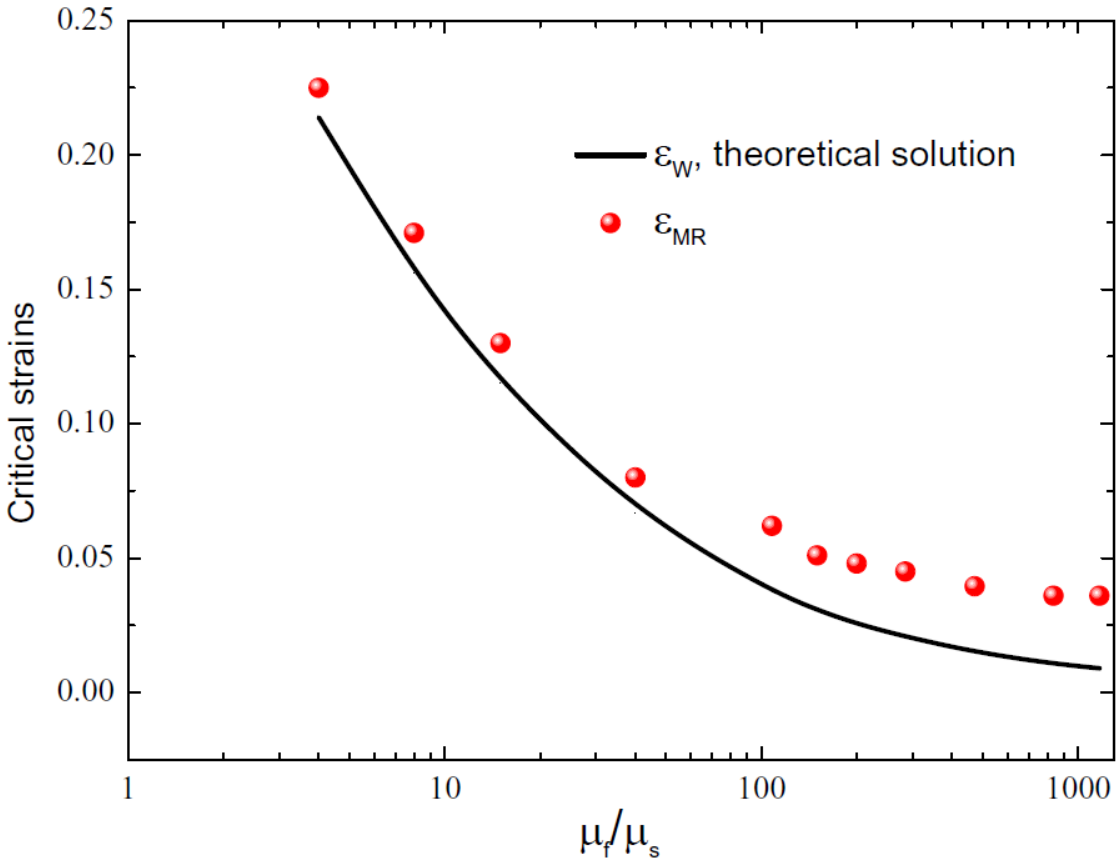

Fig. 13 Numerical simulations of the post-bifurcation modes for plane strain compression with a plane strain pre-stretch of the substrate, $\lambda_{1s}^{0} = 2$. The curve for the bifurcation strain, ε_W, at the onset of sinusoidal wrinkling is that from the theoretical calculation in Section 3.2. For this level of pre-stretch the secondary post-bifurcation mode is the mountain ridge mode (see Fig. 14) at all values of μ_f / μ_S plotted. The compressive strain at its onset is denoted by ε_{MR}. In the range where μ_f / μ_S is not large, mountain ridges form with relatively small additional compression after bifurcation. When μ_f / μ_S is large, mountain ridges form at compressive strains that are small and roughly twice ε_W.

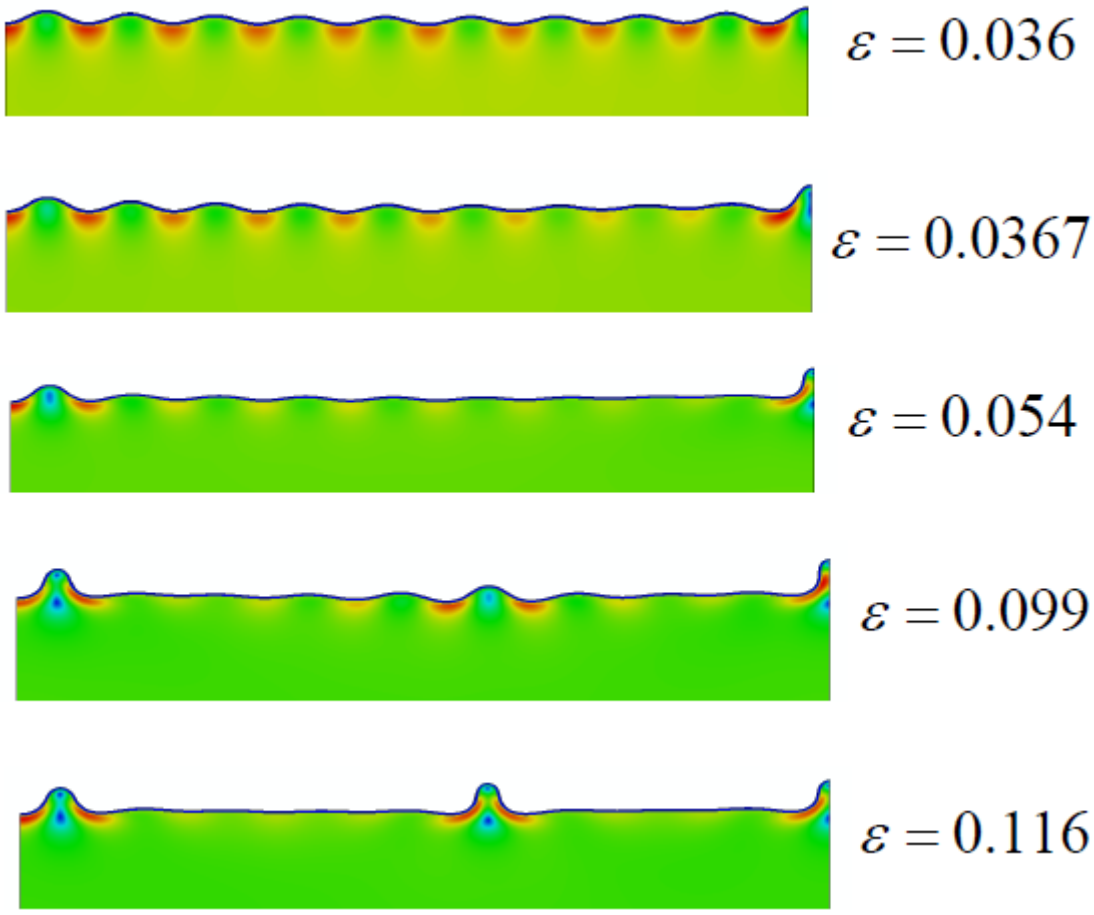

Fig. 14 Evolution of wrinkling mode under plane strain compression with a plane strain substrate pre-stretch $\lambda_{1s}^0 = 2$ for $\mu_f / \mu_S = 836$. The sinusoidal wrinkling mode associated with bifurcation at $\varepsilon_W \cong 0.01$ is stable to $\varepsilon = 0.036$ but at $\varepsilon = 0.0367$ a mountain ridge has formed at the right end of the model and the amplitude of the undulations near the ridge have been reduced. By $\varepsilon = 0.054$ a second mountain ridge is clearly forming near the left end, and by $\varepsilon = 0.099$ this ridge is fully developed with a third ridge beginning to emerge near the center. At $\varepsilon = 0.116$ three fully developed mountain ridges have formed and have relaxed the undulation amplitudes between the ridges. The ridges are a form of localization under compression.